AGU PUBLICATIONS

Geophysical Research Letters

RESEARCH LETTER

10.1002/2014GL062392

Key Points:
- We establish the relationship between return stroke speed and elve geometry
- We estimate the distribution of return stroke speeds for 55 elve observations
- The return stroke speed of elve-causative lightning is faster than expected

Correspondence to:
P. R. Blaes,
prblaes@stanford.edu

Citation:
Blaes, P. R., R. A. Marshall, and U. S. Inan (2014), Return stroke speed of cloud-to-ground lightning estimated from elve hole radii, *Geophys. Res. Lett.*, *41*, doi:10.1002/2014GL062392.

Received 30 OCT 2014
Accepted 3 DEC 2014
Accepted article online 5 DEC 2014

Return stroke speed of cloud-to-ground lightning estimated from elve hole radii

P. R. Blaes[1], R. A. Marshall[2], and U. S. Inan[1,3]

[1]Department of Electrical Engineering, Stanford University, Stanford, California, USA, [2]Department of Aeronautics and Astronautics, Stanford University, Stanford, California, USA, [3]Department of Electrical Engineering, Koc University, Istanbul, Turkey

Abstract We present the first measurements of the lightning return stroke speed that directly relate to the current return stroke, as opposed to its optical manifestation. The shape of elves is determined by the electromagnetic pulse (EMP) radiation pattern at *D* region altitudes, which is in turn controlled by the geometry and current propagation properties of the return stroke channel. In particular, numerical simulation of the EMP-ionosphere interaction shows a strong relationship between the elve "hole" radius and the current return stroke speed. The hole radii are measured from a data set of 55 elves observed with the PIPER photometer. Using these radii observations in conjunction with numerical simulations of the EMP, we perform Bayesian inference to estimate the distribution of return stroke speeds. The results show a maximum a posteriori probability return stroke speed estimate of 0.64*c* for elve producing lightning.

1. Introduction

Elves are brief optical flashes that occur in the lower ionosphere above thunderstorms. They appear as rapidly expanding rings of light with a very short time duration ($<$ 1 ms) and are a result of collisional heating of the ionospheric plasma by the intense lightning return stroke radiated electromagnetic pulse (EMP) [*Inan and Bell*, 1991; *Inan et al.*, 1997]. Elves were first observed from space aboard the space shuttle using an intensified video rate camera [*Boeck et al.*, 1992]. The first ground-based observations were performed by Fukunishi using three photometers [*Fukunishi et al.*, 1996], while the radial expansion of elves was verified by *Barrington-Leigh* [2000] using the "Fly's Eye" photometer.

The lightning return stroke is characterized by a brief current pulse propagating upward from the ground toward the cloud. A simplified "engineering model" is typically used to model this propagation. The transmission line class of models is widely used, including the basic transmission line, modified transmission line with linear altitude decay (MTLL), and modified transmission line with exponential decay (MTLE) [*Rakov et al.*, 1998]. These models are parameterized by a current pulse profile, a return stroke speed at which the pulse propagates up the channel, and an altitude decay parameter in the case of MTLL and MTLE. The current return stroke speed, which cannot be measured directly, has typically been assumed to be the same as the optical wave speed—between $\frac{1}{5}c$ and $\frac{2}{3}c$ [e.g., *Rakov*, 2007]. Recent numerical modeling of the return stroke which accounts for the thermodynamics of the channel, however, has predicted differing speeds for the optical and current pulses with the current pulse propagation being significantly faster [*Liang et al.*, 2014].

In this paper, we show that it is possible to estimate the current return stroke speed from the geometric features of elves, the optical ionospheric signatures of the return stroke EMP. Figure 1 shows the normalized radiation pattern of simulated lightning EMPs using an MTLL return stroke model with a range of return stroke speeds. We see that as the return stroke speed approaches *c*, the resulting EMP has a more upwardly directed radiation pattern. Hence, we expect that the size of the "hole" in the center of an elve emission to be correlated with the return stroke speed of the causative stroke, as faster return strokes result in a smaller null in the vertical direction. Using elve observations captured with the PIPER (Photometric Imager for Precipitation of Electron Radiation) high-speed photometer [*Marshall and Newsome*, 2008] in conjunction with a finite difference time domain model of the lightning-ionosphere interaction [*Marshall*, 2012], we are able to estimate the return stroke speed of elve causative strokes. Our results provide evidence for a return stroke speed $> \frac{2}{3}c$, in line with the results of *Liang et al.* [2014]. Indeed, we find that the return stroke speed may take on a distribution of speeds.

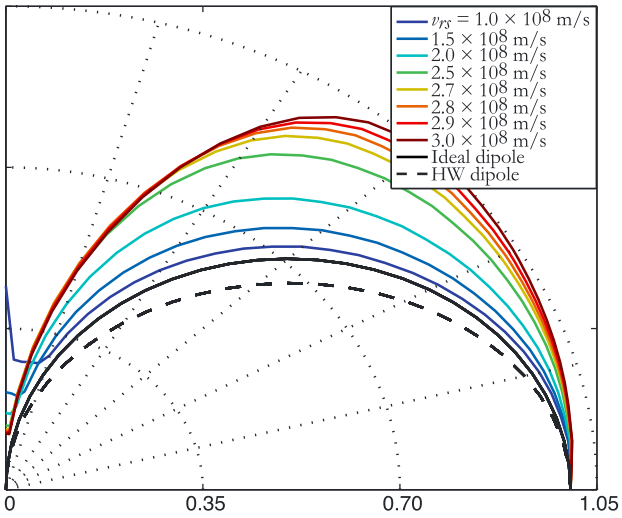

Figure 1. Normalized EMP radiation patterns simulated using the MTLL model with a range of return stroke current speeds. We observe more upwardly directed radiation patterns for return strokes with a high current wave speed.

2. Emission Profile Reconstruction

Elves appear as rapidly expanding rings of light on the lower *D* region ionosphere (~ 90 km altitude). They have a duration of less than 1 ms and have an apparent expansion rate of approximately three times the speed of light. Hence, the first photons observed by a ground-based instrument are actually emitted by the portion of the elve closest to the observer rather than from the emissions that occurred first in time. We refer to this as the "photon delay effect," and it results in significantly distorted images of elves in the field of view of ground-based instruments.

In light of the photon delay effect, it is very difficult to estimate the geometric features of elves directly from PIPER observations. Thus, we transform the PIPER data into a more natural representation which we call the "photon emission profile." This technique was first developed by *Newsome* [2010]. An example photon emission profile, along with the PIPER elve observation from which it is calculated, is shown in Figure 2. The photon emission profile displays the radial location of photon emissions relative to the center of the elve, assumed to be directly above the causative cloud to ground (CG) stroke at each point in time. The overlaid black line in Figure 2c shows the theoretical hyperbolic trajectory an elve should follow, assuming a spherical EMP expanding at *c* which is incident upon a flat ionosphere.

Several assumptions are made during the emission profile reconstruction. We assume that the elve occurs directly above the causative lightning stroke and that the elve expansion is radially symmetric. We also assume that the viewing geometry is known perfectly, including the range to the lightning, the azimuth, and the elevation angle. *Newsome* [2010, pp. 82–87] characterized the sensitivity of the algorithm to imperfectly known viewing geometries, finding that the hole radius is most sensitive to unknown elevation angle. However, our photometer included a coaxially aligned CCD camera, which allows us to measure the elevation angle accurately based on star field patterns.

The emission profiles are found using a constrained least squares reconstruction by solving the following convex optimization problem:

$$\begin{aligned} \text{minimize} \quad & ||y_s - A_s x||_2 + \lambda ||D_u x||_2 \\ \text{subject to} \quad & x \succeq 0 \\ & x^i = 0, \quad i \notin I \end{aligned} \tag{1}$$

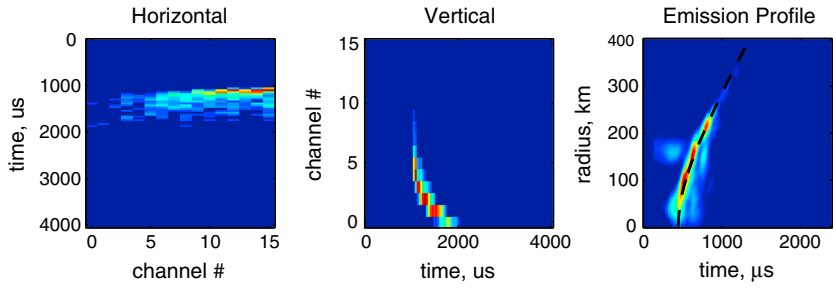

Figure 2. Example reconstructed elve emission profile. (a, b) The elve as seen in the horizontal and vertical PIPER photometers, respectively. (c) The reconstructed emission profile. The overlaid black dashed line is the trajectory followed by a spherically expanding EMP incident on a flat ionosphere at 88 km altitude.

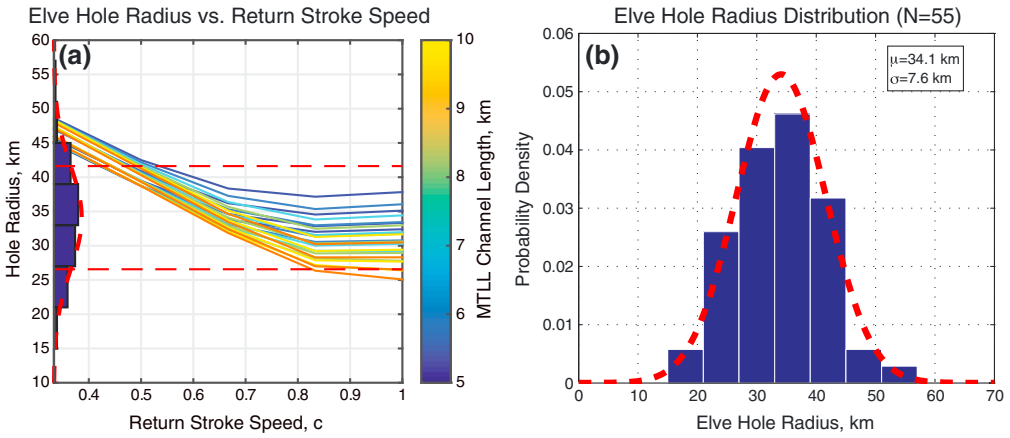

Figure 3. (a) The simulated elve hole radius as a function of return stroke speed. Other lightning parameters were varied, namely, the current wave rise time and the channel length. We see a clear relationship between faster return stroke speeds and smaller elve hole radii. Most of the remaining variation in the hole radius is due to the effective length of the channel, as is shown in the colored line plots. (b) A histogram of hole radii extracted from elves observed during the 2013 field campaign at Langmuir Laboratory.

The first term of the objective minimizes reconstruction error. Here x is the emission profile we are solving for, and y_s is the observed elve from PIPER. The matrix A_s takes into account the known viewing geometry (location of CG along with location, pointing azimuth, and pointing elevation of PIPER) and raytraces photons from the ionosphere back onto the PIPER aperture. The second term of the objective is a regularization term which promotes smoothness in the reconstructed emission profile. The matrix D_u is a first-order finite difference operator which penalizes discontinuous jumps in the elve expansion [*Newsome*, 2010, pp. 141–142]. The regularization parameter λ controls the degree to which we promote smoothness. The constraint $x \geq 0$ is used because photons are emitted rather than absorbed, and the constraint $x^i = 0$ is used to reject noise outside of the region of interest, defined by the set of pixels I in which elve photons are present.

Once an emission profile is found, it is trivial to extract the elve hole radius. In the emission profile shown in Figure 2, the hole radius is simply the vertical offset of the profile from the radius = 0 axis. In practice, for both simulated and observed elves, we take the hole radius to be the radius at which the time-integrated emission profile reached 50% of its peak.

3. Data Set

Our elve observations were collected using the PIPER high-speed photometer [*Marshall and Newsome*, 2008] at Langmuir Laboratory, New Mexico, during the summer of 2013. The PIPER instrument contains two 16-anode photomultiplier tube (PMT) arrays oriented orthogonal to one another, allowing the spatial distribution of transient luminous events to be observed. Each PMT is sampled at 25 kHz, fast enough to temporally resolve the brief (< 1 ms) elve emissions. One example elve observation is shown in Figures 3a and 3b.

During the 2013 lightning season, we observed hundreds of elves from Langmuir Laboratory. However, we find that the elve hole can only be observed and reliably measured under a narrow range of conditions. If the elve is too close, then light from the causative CG may be in the field of view and obscure the hole. On the other hand, if it is too far away (> 600 km), then the elve will be low on the horizon and atmospheric scattering and absorption become problematic. In some instances, especially after large +CG strokes, the elve is followed by sprites and/or halos which obscure the elve hole and make emission profile reconstruction difficult. Finally, since PIPER has a 18° field of view, the center of the elve must be within 9° of the field-of-view center in order for the hole to be measurable.

Of the hundreds of elves observed in 2013, 55 had the appropriate viewing conditions to make hole radius measurements possible and were not followed by sprites or halos. A histogram of the extracted elve hole radii from these observations is shown in Figure 3b.

4. Return Stroke Speed Estimation

We consider three parameters of the lightning return stroke, under a MTLL propagation model, which have a significant effect on the elve hole radius—the return stroke speed, channel length, and the current pulse rise time:

$$\theta = [v_{RS} \;\; \ell_{chan} \;\; \tau_r]^T \tag{2}$$

These three parameters are swept in the numerical EMP model over a realistic range of values and the resulting elve hole radii are extracted. A traditional exponential ionosphere from *Wait and Spies* [1964] is used with $h' = 88$ km and $\beta = 0.5$. The results of these simulation runs are shown by the colored curves Figure 3a. Each of the curves shows the hole radius as a function of return stroke speed with different choices of channel length and rise time. It is clear from these simulations that return stroke speed is the dominant factor in determining the elve hole radius. The parameter accounting for most of the remaining observed variation is the channel length, which determines the altitude decay rate for MTLL. We perform a quadratic fit on these results to produce an analytical model giving an estimated hole radius for a given set of return stroke parameters, denoted by $r_{model}(\theta)$.

Assuming Gaussian errors in the radius measurement from data, the likelihood of a given radius measurement is normally distributed according to

$$r_{meas}|\theta, \sigma \sim \mathcal{N}\left(r_{meas} - r_{model}(\theta), \sigma^2\right) \tag{3}$$

Here r_{meas} is the measured radius estimate and σ^2 is the variance of the measurement. Now, using this likelihood function in conjunction with "reasonable" prior probabilities for the lightning parameters, we use Bayes' rule to estimate the joint posterior probability for the three parameters

$$p(\theta, \sigma|r_{meas}) = \frac{p(r_{meas}|\theta, \sigma)p(\theta, \sigma)}{\int p(r_{meas}|\theta, \sigma)p(\theta, \sigma)\mathrm{d}\theta\mathrm{d}\sigma} \tag{4}$$

The marginal distribution for the return stroke speed, given our observed elve hole radii, is then

$$p(v_{RS}|r_{meas}) = \iiint p(\theta, \sigma|r_{meas})\mathrm{d}\ell_{chan}\mathrm{d}\tau_r\mathrm{d}\sigma \tag{5}$$

Rather than numerically integrate these four-dimensional integrals, we estimate the posterior distribution by performing Markov Chain Monte Carlo (MCMC) sampling [*Foreman-Mackey et al.*, 2013]. This approach uses a large number of Markov chains which take a random walk in model parameter space, providing an estimate of the underlying density.

As little is experimentally known about the actual distributions of the return stroke parameters, we assume uniform prior probabilities over reasonable ranges for the return stroke speed, current rise time, and channel length. This can be thought of as a noninformative choice of priors which does not bias the resulting model posterior probability. We assume that return stroke speed varies between $\frac{1}{3}c$–c. Current rise time is assumed to vary between 1μs and 7μs, a reasonable choice for first return strokes [*Rakov and Uman*, 2003]. Channel length is assumed to vary between 5 km and 10 km. Finally, σ is assumed to be distributed as a Jeffreys prior, $p(\sigma) \propto \frac{1}{\sigma}$, a standard noninformative prior for the variance of Normal distributions [*Gelman et al.*, 2013]. While estimating the posterior density through MCMC sampling, we used 200 random walkers, performed 2000 steps, and kept track of the Markov chain locations after a burn-in period of 1000 steps. Our MCMC sampler had an acceptance rate of 0.45 and an autocorrelation time of 61 steps, indicating that it properly converged and was drawing samples from the posterior distribution.

5. Results and Discussion

Our estimated posterior distribution of elve-causative lightning parameters is shown in Figure 4. This "corner plot" displays the parameter marginal distributions on the diagonal and the pairwise joint probabilities on the off diagonal.

Of particular interest is the panel in the top left showing the marginal probability distribution of current return stroke speed. The distribution is sharply peaked with a maximum a posteriori probability at 0.64*c*.

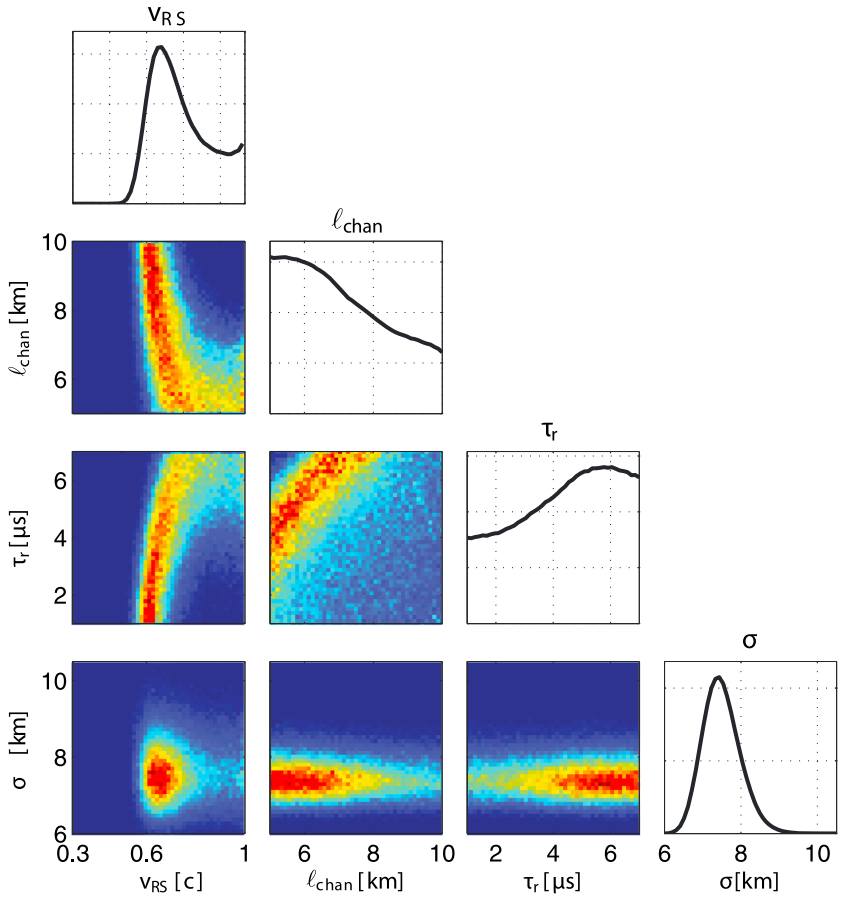

Figure 4. The posterior distribution of return stroke parameters found through MCMC sampling. This corner plot provides a convenient means of visualizing the multidimensional parameter space using only two dimensions. The diagonal line plots show the marginal distributions for the parameters, while the off-diagonal plots show the joint distribution for each pair of parameters.

This is faster than the commonly accepted range of 0.3*c*–0.5*c* [*Rakov et al.*, 1998]. Note that, according to our model, there is very low probability that an elve is produced by a return stroke with $v_{RS} < 0.5c$. This makes sense given the histogram of radii in Figure 3; a $v_{RS} < 0.5c$ implies a hole radius greater than 40 km, which we observe very few of. The distribution flattens at about 0.75*c* because the elve hole radius becomes less sensitive to v_{RS} at high speeds. This is apparent in the flattening of the line plots in Figure 3a as v_{RS} approaches *c*. Note that the weak dependence of the elve hole radius upon channel length and current rise time results in flatter posterior distributions with peaks that are not as well defined.

The uncertainty of the return stroke speed estimation in our model is tied to the width of the marginal posterior distribution. While the distribution has a maximum at 0.64*c*, we can say with 95% confidence that the return strokes in our data set had speeds between 0.52 and 0.94*c*. Additionally, we observe that the 16-50-84th percentiles of our posterior samples are 0.62-0.71-0.88*c*, respectively. Given that the viewing geometry and distance to the causative stroke used in our hole radius estimation are fairly accurate, we expect that the most significant source of physical uncertainty affecting this return stroke speed estimate is actually the effective lightning channel length (or alternatively the rate at which current decays with altitude), as this has an impact on the current moment and EMP radiation pattern.

The faster return stroke speeds estimated by our model lend credence to the results of *Liang et al.* [2014], who predicted a current return stroke speed of 0.84*c*, significantly faster than the optical speed. It is important to note that Liang et al. only simulated return strokes with initial conditions consistent with those of subsequent strokes. All elves we have observed are produced by first return strokes, which may have slower return stroke speeds due to the fact that the initial conditions of the channel include significantly

lower temperature and pressure. We further note that since elves are used to compute these return stroke speeds, these speeds may be particular to elve-producing lightning; lightning that does not produce elves may have a different distribution of return stroke speeds.

Acknowledgments
This work was supported by Defense Advanced Research Projects Agency grant agreement HR0011-10-1-0058. The data used for this study are available upon request from the authors.

The Editor thanks two anonymous reviewers for their assistance in evaluating this paper.

References

Barrington-Leigh, C. P. (2000), Fast photometric imaging of high altitude optical flashes above thunderstorms, Thesis PhD, Department of Applied Physics, Stanford Univ.

Boeck, W. L., O. H. Vaughan Jr., R. Blakeslee, B. Vonnegut, and M. Brook (1992), Lightning induced brightening in the airglow layer, *Geophys. Res. Lett.*, *19*(2), 99–102.

Foreman-Mackey, D., D. W. Hogg, D. Lang, and J. Goodman (2013), emcee: The MCMC Hammer, *Publ. Astron. Soc. Pac.*, *125*, 306–312, doi:10.1086/670067.

Fukunishi, H., Y. Takahashi, and M. Kubota (1996), Elves: Lightning-induced transient luminous events in the lower ionosphere, *Geophys. Res. Lett.*, *23*, 2157–2160, doi:10.1029/96GL01979.

Gelman, A., J. B. Carlin, H. S. Stern, D. B. Dunson, A. Vehtari, and D. B. Rubin (2013), *Bayesian Data Analysis*, CRC Press, Boca Raton, Fla.

Inan, U. S., and T. F. Bell (1991), Heating and ionization of the lower ionosphere by lightning, *Geophys. Res. Lett.*, *18*, 705–708, doi:10.1029/91GL00364.

Inan, U. S., C. P. Barrington-Leigh, S. Hansen, V. S. Glukhov, and T. F. Bell (1997), Rapid lateral expansion of optical luminosity in lightning-induced ionosphere flashes referred to as "elves", *Geophys. Res. Lett.*, *24*(5), 583–586.

Liang, C., B. Carlson, N. Lehtinen, M. Cohen, R. A. Marshall, and U. Inan (2014), Differing current and optical return stroke speeds in lightning, *Geophys. Res. Lett.*, *41*, 2561–2567, doi:10.1002/2014GL059703.

Marshall, R., and R. Newsome (2008), Fast photometric imaging using orthogonal linear arrays, *IEEE Trans. Geosci. Remote Sens.*, *46*, 3885–3893.

Marshall, R. A. (2012), An improved model of the lightning electromagnetic field interaction with the D-region ionosphere, *J. Geophys. Res.*, *117*, A03316, doi:10.1029/2011JA017408.

Newsome, R. (2010), Ground-based photometric imaging of lightning EMP-induced transient luminous events, Thesis, Stanford Univ., Stanford, Calif.

Rakov, V. A. (2007), Lightning return stroke speed, *J. Lightning Res.*, *1*(1935), 80–89.

Rakov, V. A., and M. A. Uman (2003), *Lightning: Physics and Effects*, Cambridge Univ. Press, Cambridge, U. K.

Rakov, V. A., S. Member, and M. A. Uman (1998), Lightning return stroke models including some aspects of their application, *IEEE Trans. Electromagn. Compat.*, *40*(4), 403–426.

Wait, J. R., and K. P. Spies (1964), *Characteristics of the Earth-ionosphere Waveguide for VLF Radio Waves*, U.S. Dep. of Commer., National Bureau of Standards, Washington, D. C.